Supplemental Information

Activation of RIG-I by incoming RNA virus nucleocapsids containing a 5'-triphosphorylated genome

Michaela Weber, Ali Gawanbacht, Matthias Habjan, Andreas Rang, Christoph Borner, Anna Mareike Schmidt, Stephanie Devignot, Georg Kochs, Adolfo García-Sastre, and Friedemann Weber*

Table S1

Viral system[1]	Genome polarity[2]	Genome 5'end	Attachment	Primary transcription	Genome replication / secondary transcription	Earliest step affected by CHX[3]
FLUAV	(-)	**ppp**AGCGAAAGCA... (Segment 1 of 8)	yes	yes	yes	Genome replication
VSV	(-)	**ppp**ACGAAGACAA...	yes	yes	yes	Genome replication
RVFV	(-)	**ppp**ACACAAAGAC... (3 segments)	yes	yes	yes	Primary transcription
RVFV tc-VLPs	(-)	**ppp**ACACAAAGAC... (M segment ends)	yes	yes	no	Primary transcription
ghost VLPs	none	**None**	yes	no	no	none
LACV	(-)	**ppp**ACACAAAGAC... (3 segments)	yes	yes	yes	Primary transcription
PHV	(-)	**p**UAGUAGUAGU... (3 segments)	yes	yes	yes	Primary transcription
SFV	(+)	**m7G**ATGGCGGATG...	yes	n.a.[4]	n.a.	Genome replication

[1]Virus abbreviations: FLUAV, influenza A virus; LACV, La Crosse virus; PHV, Prospect Hill virus; RVFV, Rift Valley fever virus; SFV, Semliki Forest virus; VLPs, virus-like particles; VSV, Vesicular stomatitis virus. [2](-): negative-strand RNA virus, (+): positive-strand RNA virus. [3]CHX, Cycloheximide. [4]n.a., not applicable

Fig. S1 (related to all figures)

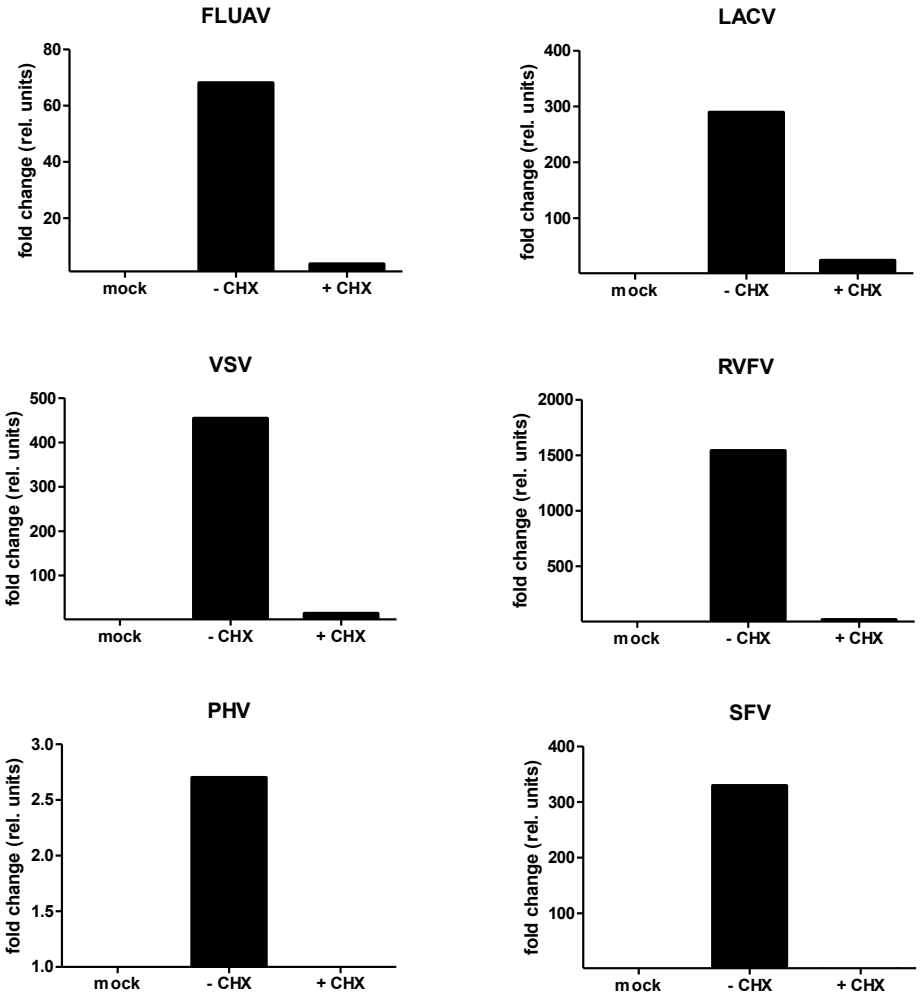

Effect of CHX treatment on viral RNA synthesis. A549 cells were either left untreated, or pretreated with CHX (50 µg/ml) for 1 h at 37°C, and infected with viruses at an MOI of 1. Seven hours (RVFV) or twelve hours (all other viruses) post-infection, cells were lysed and the total cell RNA was extracted. Viral RNA levels were measured by real-time RT-PCR as indicated in Supplementary Materials and Methods.

Fig. S2 (related to Fig. 1)

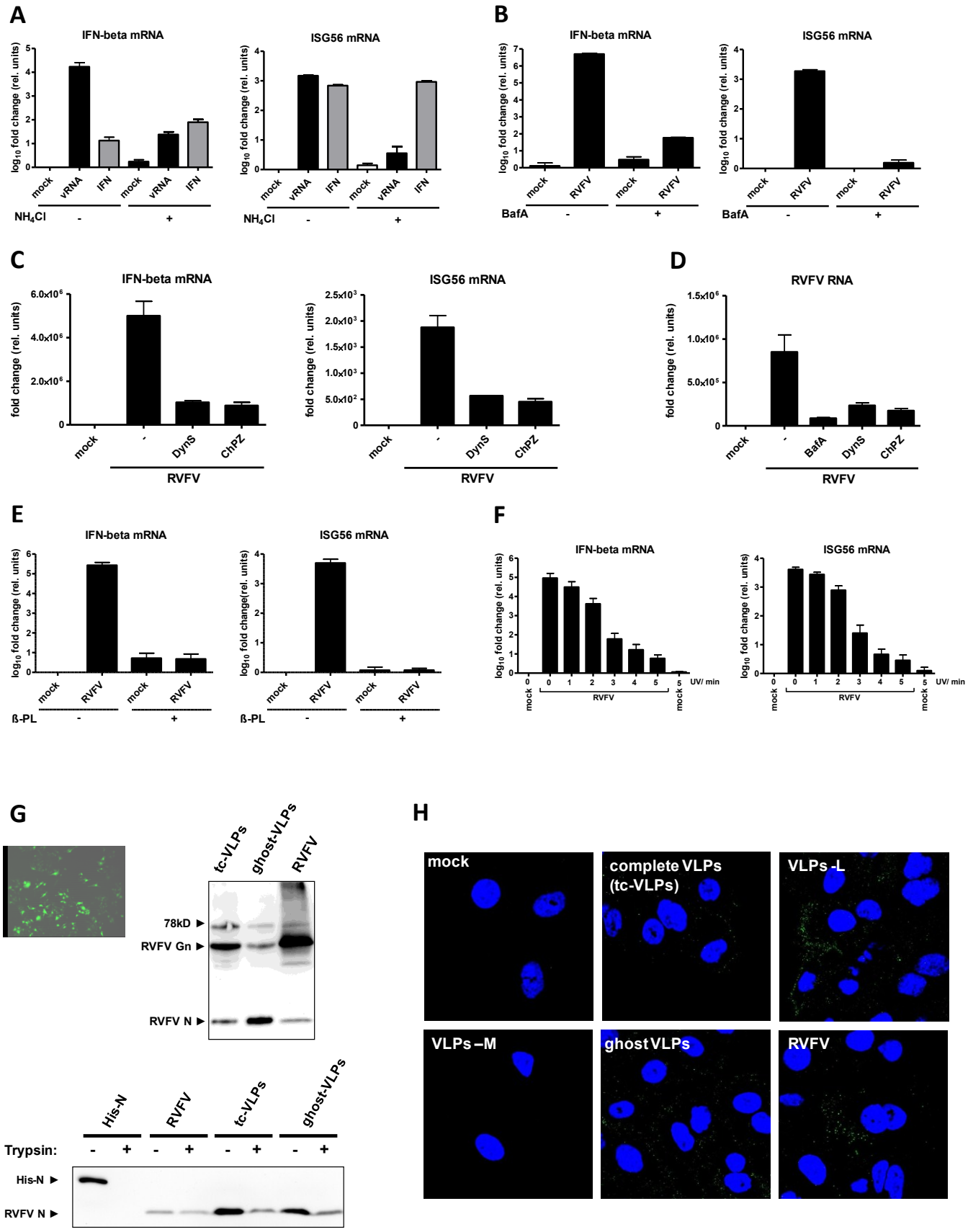

Control experiments, methods, and tools for investigating IFN induction by incoming virus particles.

(A) ISG response to IFN is unaffected by NH4Cl. A549 cells were treated for 1 h with 0 or 50 mM NH_4Cl, and then either transfected with 500 ng RNA of RVFVΔNSs::GFP particles (vRNA), or treated with 1000 U/ml IFN-α (IFN). Total cell RNA was analyzed 24 h later by real-time RT-PCR for IFN-β and ISG56 mRNA. **(B, C, and D) RVFV entry inhibitors and the IFN response**. (B) A549 cells were treated for 1 h either with 8 µl DMSO, or with 100 nM of Bafilomycin A (BafA) in DMSO, and infected and analysed as described for main Fig. 1C. (C) A parallel experiment employing 160 µM of Dynasore (DynS), or 40 µM of Chlorpromazine (ChPZ), each dissolved in DMSO. (D) Real-time RT-PCR analysis for the RVFV L gene as described (Bird et al., 2007). Note that BafA inhibits RVFV infection much stronger than DynS or ChPZ, and consequently has a more profound effect on IFN induction. **(E and F) IFN response to inactivated virus particles.** A549 cells were infected with RVFVΔNSs::GFP particles inactivated with ß-propiolactone (ß-PL) (E) or irradiated with UV (λ=311 nm) for the indicated period of time (F). **(G) Production of RVFV VLPs.** (Upper left panel) Biological activity of GFP-expressing tc-VLPs. BSR-T7/5 cells were transfected with plasmids for RVFV N and L and 24 h later infected with tc-VLPs. At 24 h post infection, GFP-positive cells were observed by fluorescence microscopy. (Upper right panel) Concentrated tc-VLPs or ghost VLPs, or cell lysate of RVFV-infected Vero cells were loaded on a 12% polyacrylamide gel and tested by immunoblot using pan-specific anti-RVFV mouse antiserum. (Lower panel) Ghost VLP preparations contain intact particles which protect the N from trypsin digestion. Recombinant RVFV nucleoprotein rN (0.2µg) containing a His-tag (His-N), as well as RVFVΔNSs::GFP, tc-VLPs, and ghost VLPs purified by ultracentrifugation were exposed to trypsin (100 µg/ml), and incubated for 30 min at 37° C. Samples were immunoblotted using an anti-RVFV N antibody. Fractions of trypsin-sensitive N indicate the presence of free N secreted by infected and transfected cells, as observed earlier (Kortekaas et al., 2011). **(H) Attachment of VLPs.** A549 cells were incubated with RVFV VLPs that are either complete (tc-VLPs), or for which either the polymerase (-L), the glycoproteins (-M), or the polymerase and the minireplicon (ghost VLPs) were omitted. RVFVΔNSs::REN infection served as positive control (RVFV). Cells were infected for 1 h at 4°C, fixed with 3% paraformaldehyde and analyzed by immunofluorescense using rabbit anti-RVFV N antiserum (1:200, green channel) and Hoechst 33342 (blue channel) as nuclear counterstain. Note that cells were not permeabilized prior to analysis. Therefore only particles attached to the cells are detected.

Fig. S3 (related to Fig. 2)

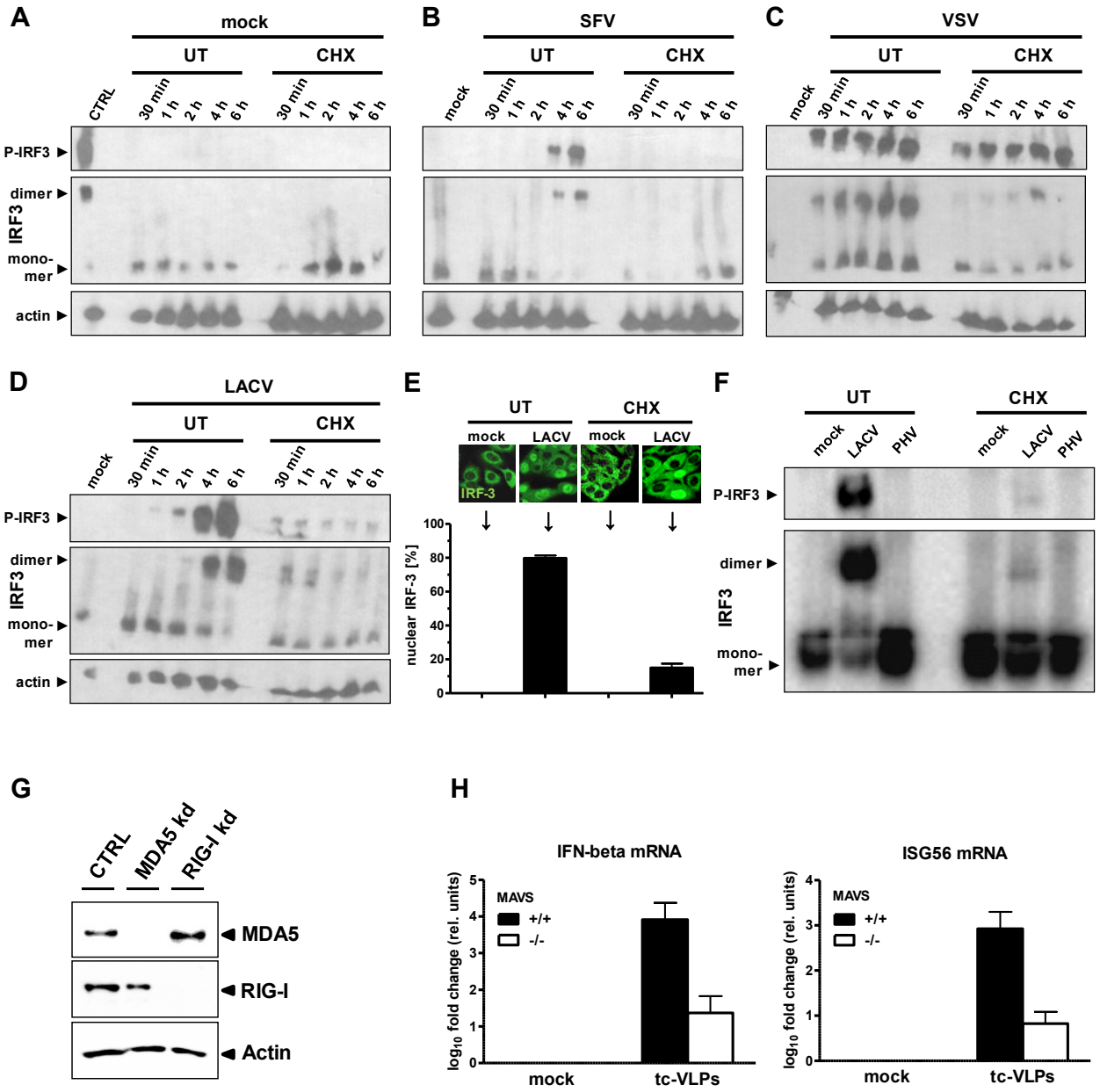

Companion experiments and controls for the influence of the 5'ppp group and RIG-I / MAVS signaling on IFN induction.

(A to F) Activation of IRF-3 in dependence of viral 5' genome ends. A549 cells were left untreated (UT) or treated with 50 µg/ml CHX. Then, cells were either mock infected (A) or infected with SFV (B), VSV (C), or LACVdelNSs (D) as described for Fig. 1. At the indicated time points post-infection, cells were lysed with RIPA buffer and protein extracts cleared from cell debris separated by native PAGE. The presence of phospho-IRF-3 (P-IRF-3) and actin, and the oligomerization state of total IRF-3 were analyzed by Western blot using

specific antisera. As internal controls, lysate from VSV-infected cells at 6 h post-infection was used as positive control for the mock infected cells (CTRL), and lysates from mock infected cells were used as negative control for the virus-infected cells. (E) Subcellular localization of IRF-3 in LACV-infected cells. A549 cells were treated with CHX or left untreated, and then mock infected or infected with LACVdelNSs. Upper panel shows representative examples of immunofluorescence analyses for IRF-3 (green). Graph shows statistics (mean and standard deviations) of the IRF-3 subcellular localization from a total of 4 independent experiments, in each of which 100 cells were randomly chosen. (F) PHV and IRF-3 activation. A549 cells were mock infected or infected with LACVdelNSs or PHV, and 6 h later monitored for IRF-3 phosphorylation and dimerisation as described for panels A to D. **(G) Knockdown of intracellular PRRs.** A549 cells were transfected with a negative control siRNA (CTRL), or with siRNAs directed against MDA5 or RIG-I. After two rounds of transfection, cells were either infected as indicated for Fig. 2B, or lysed and tested for the presence of the siRNA targets by western blot analysis. MDA5 was immunodetected using rabbit polyclonal antiserum NBP1-03299 (1:500; Novus Biologicals), actin and RIG-I were immunodetected as indicated for Fig. S8 and Fig. 3, respectively. **(H) Host response to RVFV primary transcription in MAVS knockout cells.** wt MEFs or MEFs lacking the MAVS gene were infected with transcriptionally competent RVFV VLPs expressing a GFP reporter minireplicon (tc-VLPs). After 24 h of infection, mRNA levels of IFN-β and ISG56 were determined by real-time RT-PCR.

Fig. S4 (related to Fig. 4)

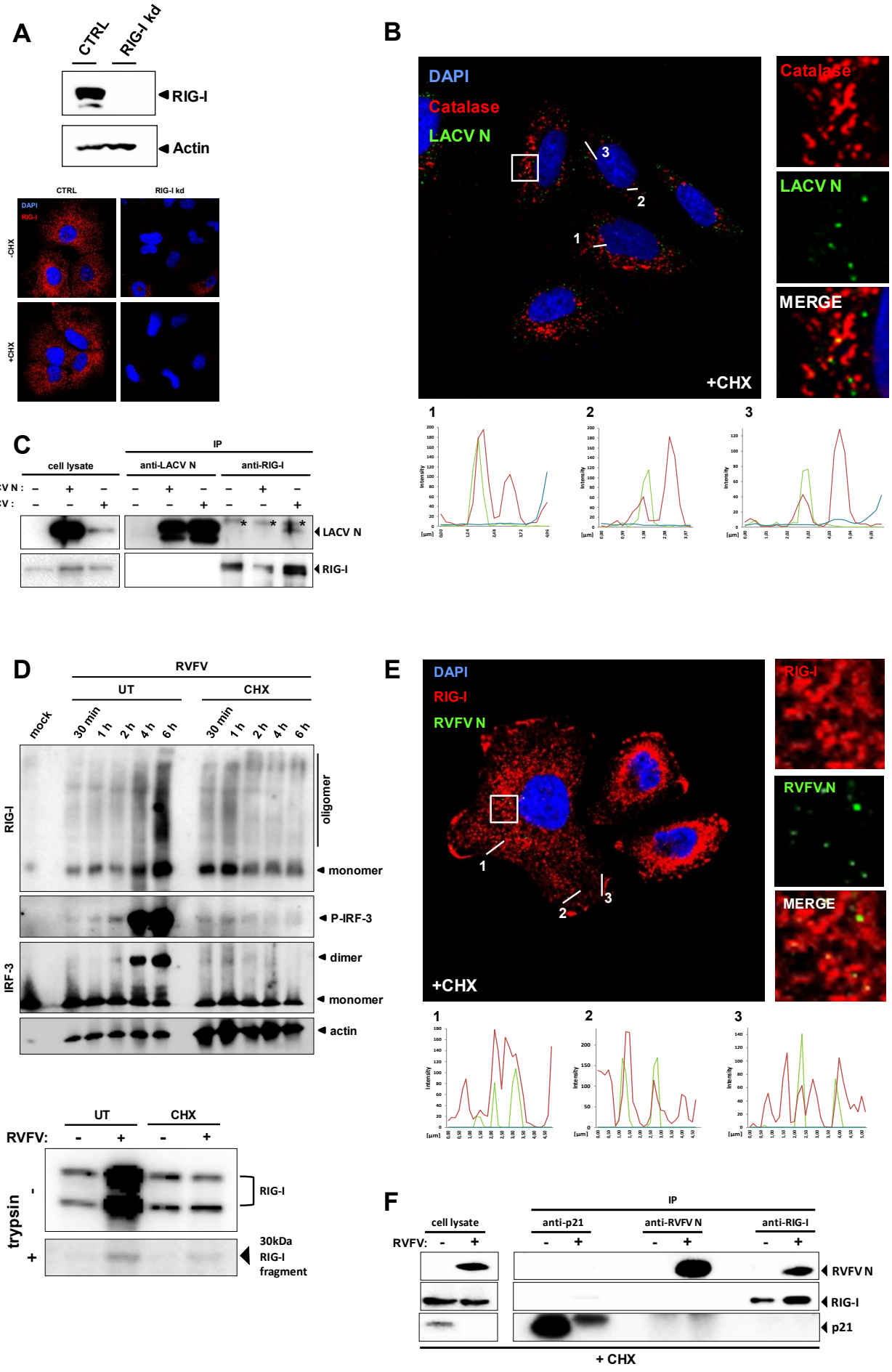

Companion experiments and controls for the interaction of RIG-I with viral nucleocapsids.

(A) RIG-I signal in knock-down cells. A549 cells were transfected with a negative control siRNA (CTRL), or with an siRNA against RIG-I. After two rounds of transfection, cells were tested for the presence of RIG-I by Western blot (upper panel) and immunofluorescence analysis (lower panel). **(B) Co-localization of LACV nucleocapsids with peroxisomes.** CHX-treated A549 cells were infected with LACVdelNSs (MOI 5) and 5 h later analyzed by immunofluorescence using rabbit and mouse antisera directed against LACV N (green channel) or catalase as a marker for peroxisomes (red channel), respectively. Cell nuclei were counterstained with DAPI (blue channel). The square area of the inset is digitally magnified on the right hand side. Three fluorescence intensity profiles (numbered 1 to 3) are shown on the bottom. **(C) Only viral nucleocapsids, but not the nucleocapsid protein alone, interact with RIG-I.** A549 cells were either untreated, transfected for 24 h with plasmid pI.18-LACV N, or infected for 5 h with LACVdelNSs (MOI of 5). Cells were lysed in RIPA buffer and subjected to immunoprecipitation (IP) for LACV N or RIG-I and analyzed by Western blot. As input control, 10% of the cell lysate were analyzed in parallel (left lanes). * indicate unspecific bands. **(D) Activation of RIG-I and IRF-3 by RVFV.** (Upper panel) A549 cells were treated with 0 or 50 µg/ml CHX and then infected with RVFVΔNSs::REN at an MOI of 5. After the indicated incubation periods, cells were lysed in PBS / 0.5% Triton X-100 and analysed for oligomerization of RIG-I and IRF-3, and for phosphorylation of IRF-3. (Lower panel) RIG-I conformational switch assay of A549 cells treated with CHX and infected for 5 h with RVFVΔNSs:REN. **(E) Co-localization of RIG-I with RVFV nucleocapsids.** CHX-treated A549 cells were infected with RVFVΔNSs::GFP (MOI 5) for 5 h and analyzed by immunofluorescence using a rabbit antiserum against RVFV N (1:5000; green channel) and mouse polyclonal antiserum against RIG-I (1:200; red channel), respectively. Cell nuclei were counterstained with DAPI (blue channel). The square area of the inset is digitally magnified on the right hand side. Three fluorescence intensity profiles (numbered 1 to 3) are shown on the bottom. **(F) Co-immunoprecipitation of RIG-I and RVFV nucleocapsids.** CHX-treated A549 cells were infected with RVFVΔNSs::GFP (MOI 5) and 5 h later lysed in RIPA buffer. Lysates were subjected to immunoprecipitation (IP) using rabbit antiserum against RVFV N (1:1000), mouse monoclonal anti-RIG-I antibody ALME-1 (1:1000), or mouse monoclonal anti-p21 (1:500). As input control, 10% of the cell lysate were analyzed in parallel (left lanes).

Fig. S5 (related to Fig. 6)

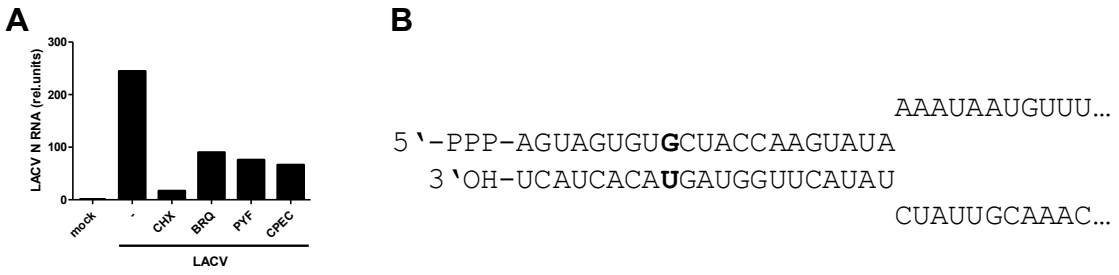

Control experiment and illustration for the activation of RIG-I by the viral panhandle. **(A) Effect of NTP withdrawal on LACV RNA synthesis.** A549 cells pretreated with different inhibitors were infected with LACVdelNSs for 5 h at an MOI of 5. Before and during the infection period, the cell culture medium contained either no additive (-), CHX (50 µg/ml) added 1 h before infection, or BRQ (10 µM, stocks dissolved in DMSO), MA (10 µM, stocks dissolved in methanol), PYF (10 µM, stocks dissolved in DMSO), or CPEC (5 µM, stocks dissolved in DMSO) added 24 h before infection. Total cellular RNA was isolated and analyzed by real-time RT-PCR using primers specific for the LACV N RNA (Verbruggen et al., 2011). **(B) LACV panhandle structure.** The first 32 nucleotides of the 5' and 3' LACV M genome segment (Genbank acc # NC_004109) are depicted as an example. Note that the non-Watson–Crick base pair G-U (bold face characters) does not disturb the dsRNA structure (Holbrook et al., 1991).

Fig. S6 (related to Fig. 7)

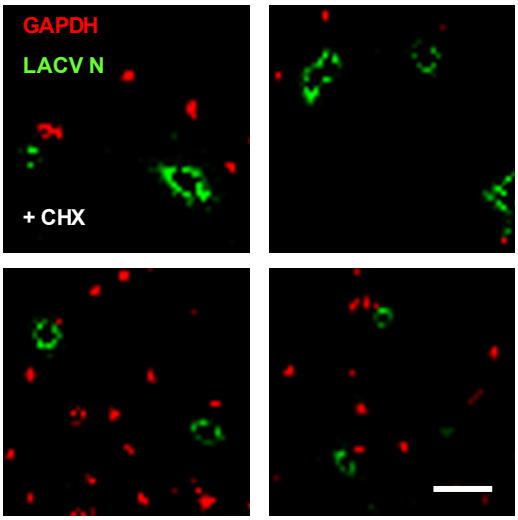

Super-resolution immunofluorescence microscopy of GAPDH and LACV nucleocapsids. A549 cells were treated with 50 µg/ml CHX and infected with LACVdelNSs (MOI 5). Cells were analyzed 5 h later by GSD double immunofluorescence using antisera against LACV N (green channel) or glyceraldehyde-3-phosphate dehydrogenase (GAPDH, red channel). The primary antibody anti-GAPDH mouse monoclonal 9B3 (HyTest) was diluted 1:100. Four example areas with nucleocapsids are shown. Scale bar 200 nm.

Supplemental Experimental Procedures

Primers for real-time RT-PCR

mRNAs of human IFN-β, ISG56, and γ-actin were measured with QuantiTect primers QT00203763, QT00201012, and QT00996415, respectively. mRNAs of murine IFN-β, ISG56, and GAPDH were measured with QuantiTect primers QT00249662, QT01161286, and QT01658692, respectively.

Short interfering RNAs

AllStar Negative Control siRNA and validated FlexiTube siRNAs (Qiagen) against RIG-I mRNA (SI03649037) and MDA5 mRNA (GS23586) were used.

Chemical inactivation of virus particles

Virus stocks containing 0.05% β-propiolactone (Acros Organics) were incubated at 4° C for 16 h. β-propiolactone was subsequently hydrolyzed by incubating samples at 37° C for 2 h.

Homodimerisation and phosphorylation of IRF-3

A549 cells were grown to 80% confluency in T25 flasks. Cell lysis and native-polyacrylamide gel electrophoresis (PAGE) were performed as described (Iwamura et al., 2001), with minor modifications. Briefly, cells were lysed in 0.5% Triton X-100 dissolved in PBS supplemented with protease inhibitor cocktail (Roche) and incubated on ice for 10 min. Lysates were sonified in a Branson 3200 Ultrasonic cleaner for 10 min at 4°C and then centrifuged at 4°C for 10 min at 10,000×g. Protein concentration was determined by Bradford assay (BioRad) and 50 μg of total protein lysate were separated by electrophoresis in a nondenaturing 8% polyacrylamide gel, with 1% sodiumdeoxycholate in the cathode buffer. Total IRF-3 and phosphorylated IRF-3 monomers and oligomers were detected by Western blot analysis with rabbit polyclonal anti-IRF-3 antibody FL-425 (1:500, Santa Cruz Biotechnology) or rabbit monoclonal anti-P386-IRF-3 (1:100, IBL), respectively. β-actin, detected by mouse monoclonal antibody 8H10D10 (1:1000, Cell signaling) served as a loading control.

Subcellular localization of IRF-3

Cells were analyzed by immunofluorescence (see Experimental Procedures) using the FL-425 rabbit polyclonal anti-IRF-3 as primary antibody (1:500, Santa Cruz Biotechnology). And goat anti-rabbit Cy2 conjugated as secondary antibody.

Real-time RT-PCR for detection of viral sequences

Total cellular RNA was isolated with the NucleoSpin RNA II kit (Macherey-Nagel) and eluted in 30 µl of ddH_2O. An aliquot of 600 ng RNA was then used as a template for cDNA synthesis. For detection of FLUAV and VSV sequences, reverse transcription was performed using the Qiagen QuantiTect® Reverse Transcription Kit using the (-) strand specific forward primers 5'-GAT AGT ACC GGA GGA TTG ACG ACT A-3' (VSV) and 5'-GGA CTG CAG CGT AGA CGC TT-3' (FLUAV). PCR was performed using QuantiTect® SYBR® Green PCR Kit and the respective forward primers, combined with the reverse primers 5'- TCA AAC CAT CCG AGC CAT TC-3' (VSV) and 5'- CAT CCT GTT GTA TAT GAG GCC CAT-3' (FLUAV). For detection of LACV, PHV and SFV sequences, the one-step QuantiTect® SYBR Green RT-PCR Kit was used. Primer sequences were 5'-GGG TAT ATG GAC TTC TGT G-3' and 5'-GCC TTC CTC TCT GGC TTA-3' (LACV S segment forward and reverse (Verbruggen et al., 2011)), 5'-CTC AAA ATT GGC AGC TAC A-3' and 5'-CTT CAC CGG CAG GCT G-3' (PHV S segment forward and reverse, and 5'-GCA AGA GGC AAA CGA ACA GA-3' and 5'-GGG AAA AGA TGA GCA AAC CA-3' (SFV nsp3 forward and reverse (Fragkoudis et al., 2008)). mRNA levels of human γ-actin were detected with QuantiTect primers QT00996415. All virus-specific values were normalized against the γ-actin mRNA signal using the ddCT method. Up-regulation of viral sequences is depicted in relation to non-stimulated, non-infected (mock) cells.

Supplemental References

Bird, B.H., Bawiec, D.A., Ksiazek, T.G., Shoemaker, T.R., and Nichol, S.T. (2007). Highly sensitive and broadly reactive quantitative reverse transcription-PCR assay for high-throughput detection of Rift Valley fever virus. J Clin Microbiol *45*, 3506-3513.

Fragkoudis, R., Chi, Y., Siu, R.W., Barry, G., Attarzadeh-Yazdi, G., Merits, A., Nash, A.A., Fazakerley, J.K., and Kohl, A. (2008). Semliki Forest virus strongly reduces mosquito host defence signaling. Insect Mol Biol *17*, 647-656.

Holbrook, S.R., Cheong, C., Tinoco, I., Jr., and Kim, S.H. (1991). Crystal structure of an RNA double helix incorporating a track of non-Watson-Crick base pairs. Nature *353*, 579-581.

Iwamura, T., Yoneyama, M., Yamaguchi, K., Suhara, W., Mori, W., Shiota, K., Okabe, Y., Namiki, H., and Fujita, T. (2001). Induction of IRF-3/-7 kinase and NF-kappaB in response to double- stranded RNA and virus infection: common and unique pathways. Genes Cells *6*, 375-388.

Kortekaas, J., Oreshkova, N., Cobos-Jimenez, V., Vloet, R.P., Potgieter, C.A., and Moormann, R.J. (2011). Creation of a nonspreading Rift Valley fever virus. J Virol *85*, 12622-12630.

Verbruggen, P., Ruf, M., Blakqori, G., Overby, A.K., Heidemann, M., Eick, D., and Weber, F. (2011). Interferon antagonist NSs of La Crosse virus triggers a DNA damage response-like degradation of transcribing RNA polymerase II. J Biol Chem *286*, 3681-3692.